Magnetic Resonance Imaging 34 (2016) 276–279

Contents lists available at ScienceDirect

Magnetic Resonance Imaging

journal homepage: www.mrijournal.com

Synergistic role of simultaneous PET/MRI-MRS in soft tissue sarcoma metabolism imaging

Xiaomeng Zhang [a,1], Yen-Lin E. Chen [a,b,1], Ruth Lim [a], Chuan Huang [a,c], Ivan A. Chebib [d], Georges El Fakhri [a,*]

[a] Gordon Center for Medical Imaging, Radiology Department, Massachusetts General Hospital, Harvard Medical School, Boston, Massachusetts 02114
[b] Department of Radiation Oncology, Massachusetts General Hospital, Boston, Massachusetts 02114
[c] Department of Radiology and Psychiatry, Stony Brook Medicine, Stony Brook, NY 11794
[d] Department of Pathology, Massachusetts General Hospital, Boston, Massachusetts 02114

ARTICLE INFO

Article history:
Received 19 August 2015
Accepted 25 October 2015
Available online xxxx

Keywords:
Simultaneous PET/MR
PET guided MR spectroscopy
Soft tissue sarcoma

ABSTRACT

The primary objective of this study was to develop and validate simultaneous PET/MRI-MRS as a novel biological image-guided approach to neoadjuvant radiotherapy (RT) and/or chemoradiation (chemoRT) in soft tissue sarcomas (STS). A patient with sarcoma of the right thigh underwent PET/MRI scan before and after neoadjuvant (preoperative) radiotherapy. The magnetic resonance imaging (MRI) and 2-deoxy-2-[-fluorine-18]-fluoro-D-glucose-Positron Emission Tomography (^{18}F-FDG-PET) scans were performed simultaneously. In the post-radiation scan, magnetic resonance spectroscopy (MRS) was subsequently acquired with volume of interest positioned in a residual hyper-metabolic region detected by PET. Post-radiation PET/MRI showed a residual T2-hyperintense mass with significantly reduced ^{18}F-FDG-uptake, compatible with near complete response to radiotherapy. However, a small region of residual high ^{18}F-FDG uptake was detected at the tumor margin. MRS of this region had similar metabolite profile as normal tissue, and was thus considered false positive on PET scan. Pathology results were obtained after surgery for confirmation of imaging findings.

1. Introduction

STS are malignant tumors that arise in any of the mesodermal tissues of the extremities (50%), trunk and retroperitoneum (40%), or head and neck (10%) [1]. The American Cancer Society estimates that in 2015 there will be 11,930 new cases and 4,870 deaths [2]; approximately 40% of patients treated with curative intent will not survive. Preoperative radiation therapy (RT) followed by limb conserving surgery has become the standard of care for truncal and extremity soft tissue sarcomas [3,4]. This standard technique for preoperative RT in the United States is established by Radiation Therapy Oncology Group (RTOG)-0630, a recently reported multi-institutional prospective phase II trial to assess late effects using preoperative image-guided radiation therapy (IGRT) [5]. In RTOG-0630, gadolinium-enhanced T1 and T2 MRI are typically used for evaluating and confirming the diagnosis. However, MRI images exhibit a variable degree of signal changes [6,7]. Changes seen by T1/T2 images are an indirect reflection of physiological but anatomic changes and thus may be nonspecific [8]. In order to evaluate tumor response, especially in STS with increased metabolic rate, metabolic imaging methods have higher sensitivity for large primary tumors and high-grade sarcoma cases [9]. Both PET and MRS have been used clinically for evaluating tumor metabolism. Although MRS is capable of detecting metabolic dysfunction in tissue that otherwise appears normal on structural imaging, most clinical applications are limited to a small region with single-voxel or multi-voxel acquisitions due to long acquisition time or SNR limitations [10]. In contrast, ^{18}F-FDG-PET can quickly outline potential metabolic abnormalities throughout the body, but may yield false positive results associated with inflammation, etc. With simultaneous MRI, ^{18}F-FDG uptake can be better localized anatomically to the tumor compared to conventional ^{18}F-FDG PET or PET-CT. With the guidance of PET, MRS can be focused on areas of most concern highlighted by the PET and provide further metabolites information on specific areas in addition to ^{18}F-FDG-PET glucose uptake. The combination of ^{18}F-FDG-PET/MRI-MRS can offer a potentially better tool to evaluate response to neoadjuvant therapy than either volumetrics or pathological percent necrosis rate. We assessed the utility of combined ^{18}F-FDG-PET/MRI-MRS in a patient

* Corresponding author at: Gordon Center for Medical Imaging, Radiology Department, Massachusetts General Hospital, Harvard Medical School, Boston, MA 02114. Tel.: + 1 617 726 9640; fax: + 1 617 726 6165.
E-mail addresses: zhang@pet.mgh.harvard.edu (X. Zhang), elfakhri@pet.mgh.harvard.edu (G. El Fakhri).
[1] Co-first authors.

http://dx.doi.org/10.1016/j.mri.2015.10.027
0730-725X/

who underwent neoadjuvant chemoradiation for a lower extremity soft tissue sarcoma.

2. Materials and methods

A 60-year-old female patient with soft tissue sarcoma of the right leg underwent simultaneous ^{18}F-FDG-PET/MR on a commercially available whole-body simultaneous PET–MR scanner (Siemens Biograph mMR, Siemens Healthcare, Erlangen, Germany) before and after preoperative radiation treatment. This scanner consists of an MR-compatible lutetium oxyorthosilicate (LSO) crystal based PET camera inside a 3 Tesla MR scanner, which provides 258 mm axial field of view and 4.4 mm full width at half maximum (FWHM) transverse spatial resolution at 1 cm off the center. The patient fasted for at least 12 hours before the ^{18}F-FDG injection for each scan and no premedication was performed. T1- and T2-weighted MRI with fat saturation and ^{18}F-FDG-PET acquisitions were performed simultaneously. In the post-radiation scan, Proton MRS was performed on tumor and normal tissue, as well as on a small region of abnormally high ^{18}F-FDG uptake at the tumor margin. Prior to the MRS acquisition, 3D shimming followed by manual shimming was performed to ensure homogeneity of the magnetic field in MRS voxels. Proton MRS was performed on three volumes of interest (VOI) using the STimulated Echo Acquisition Mode (STEAM) sequence with a repetition time of 1,500 ms, an echo time of 135 ms with 64 acquisitions and water suppression. The first two VOI ($4 \times 4 \times 4$ cm^3) were carefully positioned respectively within the tumor and normal tissue at the same location on the contralateral leg. A third VOI ($1.1 \times 1.1 \times 2.5$ cm^3) was then placed on a region with abnormal ^{18}F-FDG uptake at the tumor margin guided by fused PET/MRI images. The total acquisition time of MRS was approximately 9 min for all three VOIs.

3. Results

There is no difference observed in the size or characteristics of the tumor on MRI T2-weighted images before or after radiation treatment. In contrast, pre-radiation PET-MRI showed extensive high ^{18}F-FDG uptake within the tumor, while post-radiation PET-MRI showed significantly reduced extent and intensity of ^{18}F-FDG uptake, compatible with response to radiotherapy (Fig. 1). A small region of high ^{18}F-FDG uptake was detected at the tumor margin (Fig. 2). MRS of this ^{18}F-FDG avid region showed similar metabolite profile to the surrounding normal tissue. Choline-to-creatine ratio (Cho/Cr) within this avid region is 1.13 (Fig. 2.F, at Region F, Cho/Cr = 1.13), which is comparable to that of normal tissue in contralateral site (Fig. 2.D, at Region D, Cho/Cr = 1.30), but much lower than the residual tumor (Fig. 2.E, at Region E, Cho/Cr = 2.43). Therefore the small region of high ^{18}F-FDG uptake was considered a false positive on PET scan. This was later confirmed by pathology showing no viable cells in the ^{18}F-FDG avid region (Fig. 3). MRS performed at the tumor core demonstrated increased choline levels, which is a sign of higher membrane turnover, compared to the spectrum obtained from normal tissue. Radiation-induced cell-death prevents glucose transportation across cell membranes, resulting in no ^{18}F-FDG uptake in treated tumor. However, radiation damage may take weeks to break down cell membranes that are reflected by the high choline level on MRS. Pathology results were obtained after surgery for confirmation of imaging findings. The gross specimen consisted of a $9.5 \times 8.5 \times 6.2$ cm well-circumscribed mass showing areas of necrosis and cystic degeneration, surrounded by skeletal muscle and fibroadipose tissue. Histologically, the tumor showed no specific line of differentiation and was diagnosed as an undifferentiated pleomorphic sarcoma (UPS). The tumor showed scattered single highly pleomorphic cells, with 98% of the tumor replaced by necrosis and fibrosis. The area corresponding to the small region of ^{18}F-FDG uptake but negative on MRS was indeed necrotic. The combined PET and MRI-MRS therefore provided complementary information on the tumor response.

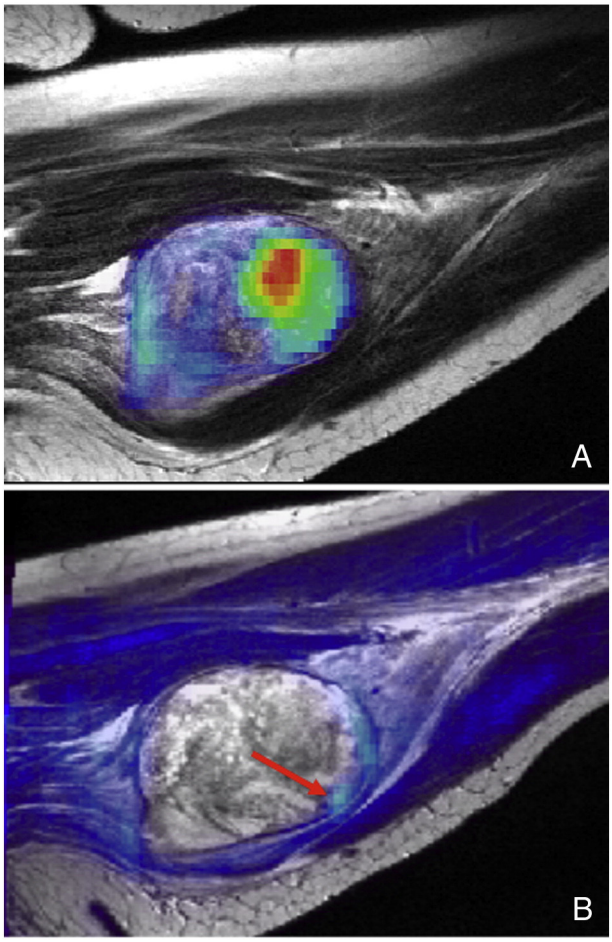

Fig. 1. A. Pre-radiotherapy fused PET and T2-W MRI. B. Post-radiotherapy fused PET and T2-WMRI. On T2-weighted MR, the initial tumor and edema margins extend beyond the region of high ^{18}F-FDG uptake. Pathology of the excised tumor found malignant cells corresponding only to the regions of abnormally high ^{18}F-FDG uptake. On post-radiotherapy scans, residual high ^{18}F-FDG uptake (red arrow) was demonstrated by MRS and confirmed by pathology, to represent post-radiation inflammation rather than residual tumor.

4. Discussion

Currently T1 (with and without contrast) and T2 MRI sequences are used routinely to assess soft tissue sarcomas. However, it is difficult to assess treatment response using MRI because most soft tissue sarcomas do not show significant changes in size when comparing pre- to post- radiation imaging. Metabolic imaging with MRS or ^{18}F-FDG-PET has shown higher sensitivity and specificity in a variety of cancers. MRS is capable of simultaneous measurement of multiple metabolites. Therefore, MRS is often used in situations where other medical imaging modalities are inconclusive. Since nearly all metabolites contain protons, in vivo proton MRS is a powerful technique to quantify a large number of biologically important compounds in tissue. A prominent resonance in proton spectra is choline (Cho) which is involved in pathways of phospholipid synthesis and degradation, thereby reflecting membrane turnover. Increased choline signal has been observed in cancer, Alzheimer's disease and multiple sclerosis, while increased choline levels are associated with cancer proliferation. Although MRS

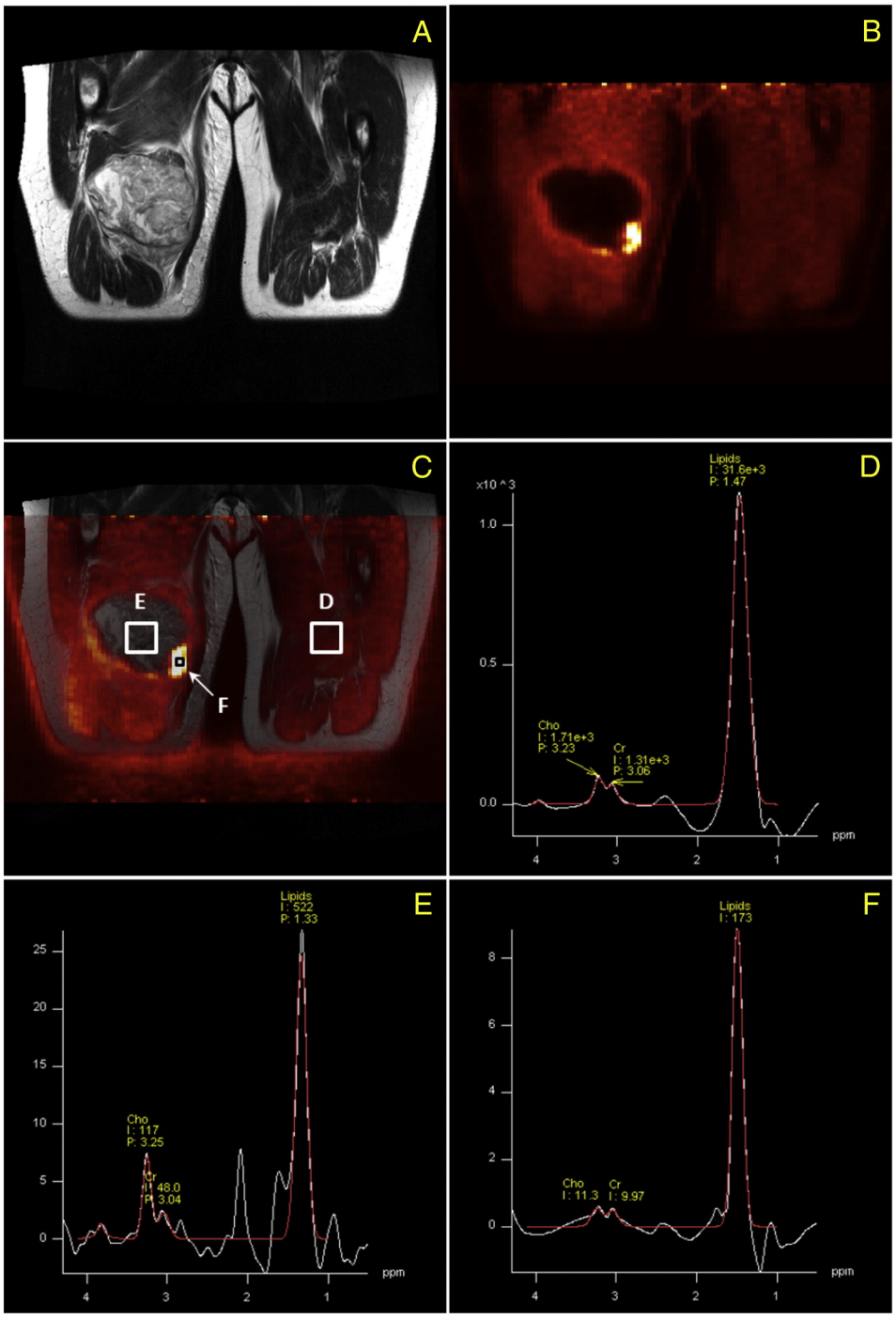

Fig. 2. PET-guided MRS can reduce ^{18}F-FDG-PET false positives by providing additional metabolite information. Post-radiotherapy T2-weighted MR image shows a residual tumor mass in the right thigh (Fig. 2.A). No abnormal ^{18}F-FDG uptake was shown on PET with the exception of a small region at the tumor margin (Fig. 2.B). MRS volumes of interest were placed at i) the center of the residual tumor tissue ($4 \times 4 \times 4$ cm) (Fig. 2.C, Region E), ii) normal tissue ($4 \times 4 \times 4$ cm) (Fig. 2.C, region D) and iii) the ^{18}F-FDG-avid region ($1.1 \times 1.1 \times 2.5$ cm) (Fig. 2.C, region F). Choline-to-creatine ratio (Cho/Cr) within the residual tumor is 2.43 (Fig. 2.E, at region E), which is higher than the ratio in normal tissue (Fig. 2.D, at region D, Cho/Cr = 1.30), and also higher than the ratio in the ^{18}F-FDG-avid region (Fig. 2.F, at region F, Cho/Cr = 1.13). Cho/Cr ratio of the ^{18}F-FDG-avid region that is comparable to that of normal tissue suggests a false positive ^{18}F-FDG-PET scan for tumor metabolism, which was confirmed by pathology result after surgery. MRS data were processed by Siemens Syngo and lc-model. Post-processing steps include water reference processing, FID shifting, zero-filling, baseline correction, phase correction and curve fitting.

allows non-invasive measurement of selected metabolites in vivo, recent evidence suggests that metabolic abnormalities in cancerous tumors are characterized by the heterogeneity of the distribution rather than absolute concentrations of one or more metabolites [11]. Most clinical applications of proton MRS are limited to single-voxel spectroscopy or low resolution chemical shift imaging (CSI) because of the long acquisition times required by MRS due to the intrinsic low concentrations of these metabolites compared to protons in water. This limitation can be overcome by using novel integrated PET/MRI systems. With its sensitivity and whole body capability, PET can quickly highlight the location of potential metabolic abnormalities. MRS can then be performed at those regions of interest as in the case presented. Potential applications of simultaneous PET-MRI-MRS can also be expanded to other cancers where assessing treatment response

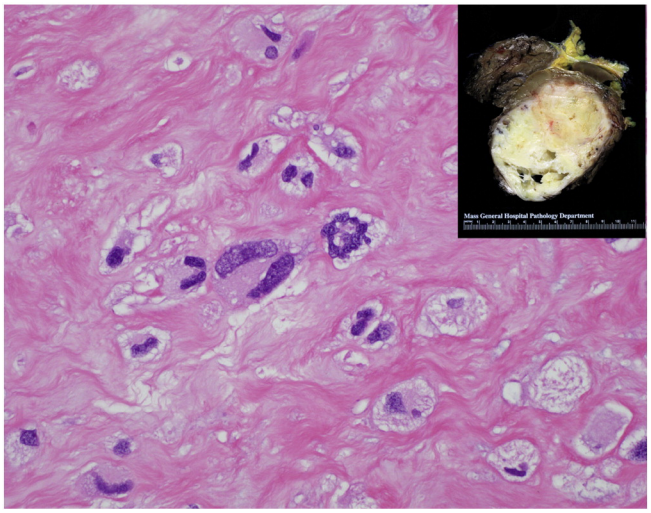

Fig. 3. The tumor is grossly well-circumscribed, composed of mostly white solid fibrous areas and scattered foci of necrosis and cystic degeneration, surrounded by skeletal muscle and fibroadipose tissue. Histologically, the tumor was largely replaced by necrosis and fibrosis with scattered highly pleomorphic cells scattered throughout (hematoxylin and eosin, 400×).

may be difficult using traditional anatomic imaging, including gliomas, bone tumors, gastrointestinal cancer, and others. The MRI obtained simultaneously with ^{18}F-FDG-PET provides superior soft tissue anatomic detail than PET-CT. The ^{18}F-FDG-PET can be used for the detection of enhanced glucose metabolism in these tumors, while MRS provides more specific information about metabolite concentrations at areas where tumor may be difficult to differentiated from inflammation/scar/necrosis. This combination provides potentially more accurate information for assessment of response to therapy. PET/MRI-MRS could potentially also be useful for imaging-guided radiation to escalate treatment dose to residual areas of tumor after initial treatment or for image-guided surgery.

5. Conclusions

While PET can quickly identify regions with abnormal metabolism, MRS can provide additional specific metabolic information in suspicious regions. Simultaneous PET/MRI-MRS imaging can serve as a gross quantitative, in vivo analog of the postsurgical histological exam, able to classify imaged tissues as either normal, inflamed, tumor, or necrotic. Therefore, it has the potential to provide more accurate treatment response assessment in sarcoma patients with equivocal ^{18}F-FDG-PET findings.

Acknowledgments

Financial support: NIH R01CA165221; NIH T32 5T32EB013180-04.

References

[1] Adult Soft Tissue Sarcoma Treatment (PDQ®). General information about adult soft tissue sarcoma. National Cancer Institue; 2015 1.
[2] Cancer facts & figs. American Cancer Society, Inc.; 2015 4.
[3] Pisters PW, Harrison LB, Leung DH, Woodruff JM, Casper ES, Brennan MF. Long-term results of a prospective randomized trial of adjuvant brachytherapy in soft tissue sarcoma. J Clin Oncol 1996;14:859–68.
[4] Yang JC, Chang AE, Baker AR, Sindelar WF, Danforth DN, Topalian SL, et al. Randomized prospective study of the benefit of adjuvant radiation therapy in the treatment of soft tissue sarcomas of the extremity. J Clin Oncol 1998;16:197–203.
[5] Bahig H, Roberge D, Bosch W, Levin W, Petersen I, Haddock M, et al. Agreement among RTOG sarcoma radiation oncologists in contouring suspicious peritumoral edema for preoperative radiation therapy of soft tissue sarcoma of the extremity. Int J Radiat Oncol Biol Phys 2013;86:298–303.
[6] Ilaslan H, Schils J, Nageotte W, Lietman SA, Sundaram M. Clinical presentation and imaging of bone and soft-tissue sarcomas. Cleve Clin J Med 2010;77(Suppl. 1):S2–7.
[7] Kroon HM, Bloem JL, Holscher HC, van der Woude HJ, Reijnierse M, Taminiau AH. MR imaging of edema accompanying benign and malignant bone tumors. Skeletal Radiol 1994;23:261–9.
[8] Landa J, Schwartz LH. Contemporary imaging in sarcoma. Oncologist 2009;14:1021–38.
[9] Hicks RJ, Toner GC, Choong PF. Clinical applications of molecular imaging in sarcoma evaluation. Cancer Imaging 2005;5:66–72.
[10] Horska A, Barker PB. Imaging of brain tumors: MR spectroscopy and metabolic imaging. Neuroimaging Clin N Am 2010;20:293–310.
[11] McIntyre DJ, Madhu B, Lee SH, Griffiths JR. Magnetic resonance spectroscopy of cancer metabolism and response to therapy. Radiat Res 2012;177:398–435.